Emerald Rapid Prototyping Journal



# Edge quality in Fused Deposition Modeling: I. Definition and analysis



| | |
|---|---|
| Journal: | *Rapid Prototyping Journal* |
| Manuscript ID | RPJ-02-2016-0020.R1 |
| Manuscript Type: | Original Article |
| Keywords: | Fused deposition modelling, accuracy |

# Edge quality in Fused Deposition Modeling: I. Definition and analysis

**Abstract**

*Purpose* – To discuss the problem of the geometric accuracy of edges in parts manufactured by the FDM process, as a preliminary step for an experimental investigation.
*Design/methodology/approach* – Three geometric variables (inclination, included and incidence angle) were defined for an edge. The influence of each variable on the geometric errors was explained with reference to specific causes related to physical phenomena and process constraints.
*Findings* – Occurrence conditions for all causes were determined and visualized in a process map, which was also developed into a software procedure for the diagnosis of quality issues on digital models of the parts.
*Research limitations/implications* – The process map was developed by only empirical considerations and does not allow to predict the amount of geometric errors. In the second part of the paper, experimental tests will help to extend and validate the prediction criteria.
*Practical implications* – As demonstrated by an example, the results allow to predict the occurrence of visible defects on the edges of a part before manufacturing it with a given build orientation.
*Originality/value* – In literature, the geometric accuracy of additively manufactured parts is only related to surface features. The paper shows that the quality of edges depends on additional variables and causes to be carefully controlled by process choices.

**Keywords**

Additive manufacturing; fused deposition modeling; edge quality; geometric accuracy; defect prediction.

## 1 Introduction

Additive manufacturing (AM) techniques allow the production of parts with complex shapes with minimum impact on build time and cost. The countless types of possible part features often involve the presence of edges with complex and variable profiles, which deserve special attention as either functional features (e.g. sharp edges of blades), decorative features (e.g. bend lines of enclosures), or ubiquitous elements of part exterior (e.g. edges of lattice structures). For plastic parts, edges do not raise safety concerns and are usually kept in the as-built state; it is thus essential that an AM process can yield good-quality edges without the need of filleting or chamfering them.
In a narrow sense, edge quality can be broadly associated with geometric accuracy, because geometric errors on edges need to be controlled within limits that do not affect part appearance and function. Edge accuracy is less of an issue for processes relying upon laser or high-definition imaging devices for material consolidation; in those cases, however, good detail resolution is usually paid with long cycle times, high equipment cost and limited choice of build materials. On the opposite side, extrusion-based processes allow the use of functional materials and less expensive machines but their limited resolution demands special attention to the control of geometric errors.
This paper focuses on the Fused Deposition Modeling (FDM) process, which builds parts layerwise by extruding two thermoplastic resins (a build material and a support material) through heated vertical nozzles (Fig. 1). The extrudate is deposited on a horizontal build platform along a piecewise linear toolpath that scans a whole cross section of the part, previously calculated by a software procedure (slicing). After a layer has been completed, the platform is lowered by a fixed distance (layer thickness) to allow the deposition of a new layer. The two extruders and the build platform are enclosed in a heated chamber to reduce thermal

gradients during cooling from extrusion temperature and avoid warping of the part. As in other AM processes, the size of form details on built parts is limited to a minimum of 2-3 times the layer thickness, which can be set to different values (typically 0.178, 0.254 and 0.330 mm) in order to achieve the desired balance of detail resolution and build time.

In literature, the accuracy of FDM parts has been widely studied (Turner and Gold, 2015) considering different types of deviations. Dimensional errors have been measured on benchmark parts representing typical geometries. Some of them include primitive shapes such as cylinders, prisms or blocks (Ziemian and Crawn, 2001; Nancharaiah *et al.*, 2010; Noriega *et al.*, 2013), possibly arranged so as to capture the dependence on build orientation (Pérez, 2002; Wang, Lin *et al.*, 2007). Some other are nonfunctional parts including features with different shapes and sizes (Bakar *et al.*, 2010; Johnson *et al.*, 2014), or even functional parts from mechanical assemblies (Singh, 2014). Collected data are usually processed to evaluate tolerance grades for given types of features.

More attention has been given to geometric errors on part surfaces. Residual strains due to differential shrinkage have been measured on samples with embedded sensors (Kantaros and Karalekas, 2013). Their overall effect is warping, which has been analyzed by either finite-element solution of continuity equations (Zhang and Chou, 2008; Xinhua *et al.*, 2015), closed equations based on simplifying assumptions (Wang, Xi *et al.*, 2007), and statistical models from experimental tests on process variables (Sood *et al.*, 2009). Predictive models have been applied to the selection of process parameters to achieve an optimal trade-off of warping with build time (Peng *et al.*, 2014).

Other causes of geometric errors have been studied for the FDM process, usually for compensation purposes. Positioning errors due to machine feed drives have been calculated (Agrawal and Dhande, 2007) and measured (Tong *et al.*, 2008) in order to decompose them into translational, rotational and scale errors on individual axes. Form and position errors due to poor flatness of the layering plane have been measured and predicted by statistical models (Boschetto and Bottini, 2014). Profile errors on planar contours of flat parts, resulting from both shrinkage and positioning errors, have been investigated through experimental plans on FDM process variables (Chang and Huang, 2011). Other experimental investigations have focused on systematic deviations due to slicing (Chen and Feng, 2011) and propagation of flatness errors from the lowermost support layers (Volpato *et al.*, 2014).

Surface finish has also received attention due to its obvious relevance to both function and appearance. Some studies analyze process-independent geometric parameters such as the volume (Masood *et al.*, 2000) and the height (Ahn *et al.*, 2005) of surface asperities; they allow first-approximation estimations of roughness as a function of surface orientation assuming theoretical profiles for the layers (Ahn *et al.*, 2009). Some other rely upon roughness measurements on samples built with different orientations, layer thicknesses and combinations of process variables (Anitha *et al.*, 2001; Campbell *et al.*, 2002; Mahapatra and Sood, 2012, Boschetto *et al.*, 2012). Accuracy and surface finish data can be used in process planning for diagnostic and optimization purposes: methods proposed for this task are based on either process-independent quality measures (Rattanawong *et al.*, 2001), roughness data (Thrimurthulu *et al.*, 2004, Boschetto *et al.*, 2013; Taufik and Jain, 2016) and multi-objective functions balancing roughness with build time and cost (Ghorpade *et al.*, 2007; Ingole *et al.*, 2011). Roughness data have also been collected to demonstrate the feasibility of improving surface finishing through machining (Pandey *et al.*, 2003), barrel finishing (Boschetto and Bottini, 2015) and chemical treatments (Galantucci *et al.*, 2009; Garg *et al.*, 2016).

It is apparent from the above review that the quality achievable in the FDM process, as in all AM processes, has been mostly associated to part surfaces. No consideration seems to have been given to edges, which are just treated as generic form details subject to the resolution limitations of the process. However, geometric errors on edges may have specific relevance for some applications. For machine parts, international standards define the possible deviations from nominal edge geometry (state of an edge) and the related design specifications (ISO, 2000). In other contexts, the profile of an edge must be carefully inspected to detect initial accuracy and degradation due to wear. The cutting edge radius of machining tools requires in-process measurement techniques based on laser triangulation (Osawa *et al.*, 2012) or image processing (Lim and Ratnam, 2012). The sharpness of cutting blades for soft materials has been studied with the aim of defining geometric requirements for the edges (Reilly *et al.*, 2004; McCarthy *et al.*, 2010) and developing indirect measurement techniques (Marsot *et al.*, 2007). Less attention has been paid to the visual perception of edge quality, which may be interesting for many applications of AM processes.

This two-part paper provides a first analysis of the geometric accuracy of edges in FDM parts. The objective of Part I is to understand whether the problem has any distinctive features compared to analogous studies related to part surfaces: as it will be discussed in the following, there are significant differences regarding both the causes of defects and the influence factors related to part geometry and build orientation. The results of this analysis have allowed to develop a process map in both graphical and procedural forms. By using the map with a given part model, critical conditions for edge quality can be readily predicted for diagnosis purposes at process planning stage.

## 2 Geometric properties of an edge

Edges of AM parts have often complex, three-dimensional shape; therefore, their geometric properties and the resulting accuracy are expected to vary from point to point. This paper will only consider straight-line edges with uniform geometric properties, assuming that the amount of geometric errors on an edge at a given point is equal to the one observed along a uniform straight-line edge with equivalent geometric properties. It is believed that such assumption does not involve any loss of generality because the input to all AM processes is a triangle mesh in STL format, where a curved edge is approximated by a sequence of short straight-line segments.

Fig. 2a shows an edge and its adjacent facets, whose outward-pointing normal unit vectors are denoted by $\mathbf{n}_1$ and $\mathbf{n}_2$. The edge has two characteristic unit vectors, the tangent $\mathbf{t}$ and the outward-pointing normal $\mathbf{n}$:

$$\mathbf{t} = \frac{\mathbf{n}_1 \wedge \mathbf{n}_2}{\left|\mathbf{n}_1 \wedge \mathbf{n}_2\right|} \quad , \qquad \mathbf{n} = \frac{\mathbf{n}_1 + \mathbf{n}_2}{\left|\mathbf{n}_1 + \mathbf{n}_2\right|}$$

Let $\mathbf{k}$ denote the unit vector in the vertical build direction, i.e. the upward-pointing normal to the horizontal build platform. By properly selecting the order of $\mathbf{n}_1$ and $\mathbf{n}_2$ in the vector product, it is assumed that the tangent vector points upwards, i.e. $\mathbf{t} \cdot \mathbf{k} \geq 0$.

From the above unit vectors, three characteristic angles can be associated to the edge as shown in Fig. 2b-c:

- the angle $\alpha$ of the tangent to the horizontal plane (inclination angle):

$$\sin\alpha = \mathbf{t} \cdot \mathbf{k} \qquad \left(0 \leq \alpha \leq 90°\right) \tag{1}$$

- the angle $\gamma$ of the normal to the horizontal plane (incidence angle):

$$\sin\gamma = \mathbf{n} \cdot \mathbf{k} \qquad \left(-90° \leq \gamma \leq 90°\right) \tag{2}$$

- the angle $\beta$ between the two facets (included angle), which is defined in the plane normal to the edge and is independent of the build orientation:

$$\sin\frac{\beta}{2} = \frac{\left|\mathbf{n}_1 + \mathbf{n}_2\right|}{2} \qquad \left(0 \leq \beta \leq 180°\right) \tag{3}$$

As the facet normals are explicitly stored in an STL model, the edges of a part can be located by selecting the triangle sides having $\beta$ below a given threshold (conveniently lower than 180°). For any build orientation, $\alpha$ and $\gamma$ can then be calculated for each edge segment. Further information on the triangles can help to recognize possible concave edges (180° ≤ $\beta$ ≤ 360°), which share the same expressions of the three angles but will not be considered in this work.

While $\beta$ can be chosen independently of the other two angles, the limits of $\gamma$ depend on the value of $\alpha$ due to the perpendicularity between **t** and **n**. It is easily verified (Fig. 3a) that

$$|\gamma| \leq 90° - \alpha$$

This gives the domain of the triples ($\alpha$, $\beta$, $\gamma$) depicted in Fig. 3b, where the allowable range of $\gamma$ gets smaller and smaller with increasing $\alpha$ until it degenerates to a single value ($\gamma = 0$) for $\alpha = 90°$.
Each of the angles is likely to influence the accuracy of an edge. A small $\alpha$ may result into a visibly stair-stepped edge; a negative $\gamma$ requires support structures which may leave visible marks on the edge; a small $\beta$ may prevent the toolpath from closely following the layer contour at an edge. For a given layer thickness, it is thus assumed that the geometric errors on an edge depend only on the values of $\alpha$, $\beta$ and $\gamma$.
In the following, the influence of the three variables will be discussed in more detail considering the following two types of geometric errors:

- the position error $E_P$, defined as the average distance of the points of the actual profile of an edge from the nominal profile along a given measurement length;
- the form error $E_F$, defined as the standard deviation of the distance of the actual profile from the nominal profile.

## 3 Causes of geometric errors

The position and form errors on edges include both systematic and random components. The systematic errors will be identified as those depending on $\alpha$, $\beta$ and $\gamma$, while the random errors will be attributed to either disturbance factors or unknown effects related to the chosen process settings. The relative importance of the two error components will be experimentally evaluated in Part II. For the moment, some causes of systematic errors will be discussed and related to expected effects of the geometric variables.

### *3.1 Staircase effect*

When dealing with geometric errors on surface features, it is often observed that the stacking of layers inevitably generates a periodic profile including the free boundaries of successive layers. The resulting form error, related to the amplitude of the profile, increases with the layer thickness and is thus particularly noticeable for the FDM process. The same issue is likely to be found on edges as well, and can be analyzed under the simplifying assumption that the layers have a straight-line free boundary, thus making the cycles of the profile similar to the steps of a staircase (Fig. 4a). The depth $h$ of the triangular groove corresponding to each step can be calculated as a function of the layer thickness $s$:

$$h = \begin{cases} s \cdot \cos\alpha\,, & \alpha > 0 \\ 0\,, & \alpha = 0 \end{cases}$$

Hence, the theoretical form error equals zero for vertical edges, increases with decreasing inclination angles and tends to a maximum for horizontal edges, where it has a discontinuity with zero value. Actual form errors are expected to be always greater than zero and, as the free boundary is actually a curve, vertical edges should have larger form errors than horizontal edges (Fig. 4b).

### *3.2 Support effect*

Another well-known cause of surface defects in AM parts is the need of support structures on overhanging layers, whose removal after the build process can leave visible marks on the exposed surface. Edges should also be affected by the same issue, and thus present a variation of the form error as a function of $\gamma$. When an edge points downwards ($\gamma < 0$), support structures are always needed as the edge does not rest on underlying layers (Fig. 5a). When the edge points laterally ($\gamma = 0$) or upwards ($\gamma > 0$), support structures are still required if $\beta$ is small, because in this case each layer overhangs the underlying one by an excessive distance (Fig. 5b). The combined effect of $\beta$ and $\gamma$ can be evaluated from the angle between the lower face of the edge and the vertical direction:

$$\delta = 90° - \gamma - \beta/2$$

which, depending on machine settings, can take values up to 40-60° without the need of support structures. The relevance of this effect could depend on the way supports are removed after build. The tests reported below use a break-away support material based on high-impact polystyrene (P400R), which is removed mechanically with expectedly higher risk of damaging part surface. Additional support materials available on FDM machines include acrylic copolymers and terpolymers, which are removed by dipping the part in heated water solutions of cleaning agents; it is expected that they have a lower impact on edge accuracy. Although an explicit comparison was not made in this work, experimental tests using a soluble material (SR-30) are reported in Part II.

*3.3 Radius effect*

A first edge-specific issue is related to the radius of curvature of the deposition trajectory. Assuming constant relative speed between the nozzle and the platform, the deposited material is a strand with uniform cross-section, which must suddenly change direction at an edge. Visualizations provided by the printing software suggest that the bend radius is approximately equal to the layer thickness $s$ (Fig. 6a). The distance $d$ of the outermost point of the bend to the nominal position of the edge is a first approximation of the position error. It can be easily verified that

$$d = s \cdot \left( \frac{1}{\sin \beta/2} - 1 \right), \quad 0 < \beta < 180°$$

This means that the position error should increase when $\beta$ decreases, except perhaps for edges with small included angles, where the calculation of the toolpath prevents the bend angle from dropping below a given limit (apparently close to 45°). The position error due to the radius effect should also increase when $\alpha$ decreases, because the bend angle $\beta'$ of the trajectory gets much smaller than the included angle $\beta$ for nearly-horizontal edges (Fig. 6b).

*3.4 Offset and curved-boundary effect*

Regarding the variation of $\alpha$ with the position error, an opposite effect from above can be predicted when considering the toolpath planning strategy, which is not documented but can be partially inferred by software visualizations. To keep the material within the volume of the STL model, the toolpath is probably offset from the nominal surface by a distance close to half the width $w$ of the strand. Moreover, the free boundary of the layer is curved; for graphical convenience, its cross-section is assumed as elliptical in Fig. 7a. For vertical edges, apart from the additional offset due to the radius effect, this causes a small negative position error. For inclined edges, the layer boundaries can partially overlap the nominal profile and reduce the negative value of the position error (Fig. 7b). The effect is likely to get more pronounced for especially low values of $\alpha$.

*3.5 Slicing and swelling effects*

Two last issues may influence the position error for horizontal edges ($\alpha = 0$), which are created by a single strand of material. First, the expected vertical distance $z$ of the edge from the build platform is multiple of the layer thickness $s$, and can be systematically different from the nominal position $z_0$ of the edge; the deviation $d_1$ is given by

$$d_1 = s \cdot \lfloor z_0 / s \rfloor - z_0$$

and seems to be always negative as the calculated number of layers ($z_0$ / $s$) is rounded to the next lower integer (Fig. 8a).

Secondly, the thermoplastic resin is subject to swelling due to its visco-elastic rheology. During extrusion, the material bears a compressive strain in its cross-sectional plane; the elastic fraction of the strain is then recovered leading to expansion of the material in all transverse directions. If $\alpha = 0$, the expansion makes the part grow along $z$. The last layer retains a permanent deformation $d_2$ depending on the layer thickness and possibly to other process parameters (Fig. 8b). The two effects lead to a total position error ($d_1 + d_2$), which can be either positive or negative depending on $z_0$.

### *3.6 Additional effects*

Further error causes may be found among the ones already shown to influence surface quality. They include random variation in material properties and extrusion parameters, as well as the dynamic behaviour of machine feed drives. As a possible systematic cause, warping due to material shrinkage is also likely to have a role on edge accuracy in some conditions (parts with large size and low flexural rigidity); such issue may visibly distort long edges with simple geometries (e.g. straight-lines or circles), on which deviations from correct shape are especially apparent. Although the warping effect will not be explicitly considered in this paper, future developments will possibly extend the definition of edge quality by considering distortions as autocorrelation properties of edge profiles.

## 4 Occurrence conditions for geometric errors

The above hypotheses about error causes provide help to identify critical combinations of the angles with respect to edge accuracy. They can be summarized by the set of inequalities in Tab. 1, where the constant angles $\theta_i$ are the limits of occurrence for the different causes of geometric errors. Preliminary estimates for these parameters ($\theta_1 = 15°$, $\theta_2 = 45°$, $\theta_3 = 45°$, $\theta_4 = 60°$) lead to the process map in Fig. 9, where each of the regions highlighted in the domain of the three variables indicates the likely occurrence of an individual error cause.

The process map is equivalent to a set of preliminary rules that can help to reduce the occurrence of geometric errors on a given edge. These can be summarized as follows:

- form errors, probably more critical for their impact on function and appearance, can be reduced by avoiding: a) inclinations close to horizontal; b) incidences below a given threshold, not necessarily negative, which increases with the included angle;
- position errors can be controlled almost exclusively by avoiding small included angles, while the suggestions about inclinations to be avoided (horizontal or close to vertical) would partially conflict with the above rules related to form.

The process map can be used as a diagnostic tool in the planning phase of the FDM process. Given an STL model, the selection of the build orientation is usually driven by part geometry (e.g. if most surfaces are parallel to three reference directions) or by the need to optimize a combination of performance metrics (amount of support material, build time, build cost, average surface finish). Once the orientation has been chosen, the attention may be focused on a set of edges regarded as important for either the function or the aesthetic value of the part. For each edge, $\alpha$, $\beta$ and $\gamma$ can be calculated from the STL model, and the corresponding point can be located in the process map. If it falls in one or more critical regions, the occurrence of specific types of geometric errors can be predicted before the build.

As an application example, Fig. 10a shows the STL model of a part with size 44 × 61 × 19 mm, whose geometry results from twisting and bending operations on a ring with triangular cross section. The part has been built by the FDM process using a Stratasys Fortus 250mc machine, ABSplus-P430 model material, P400R break-away support material, and 0.254-mm layer thickness. Fig. 10b shows the built part with the support structures still attached.

The visual inspection of the edges on the built part has revealed visible geometric errors in some locations. In order to verify that the process map would have allowed to predict the occurrence of such errors, the three angles should have been evaluated in a large number of points of the properly oriented STL model. Since this is obviously impractical, a software procedure has been developed to virtually overlay the process map on the digital model of the part. The procedure first recognizes the edges of the part among all the triangle sides by comparing the normals of the adjacent facets. For each edge segment, the angles $\alpha$, $\beta$ and $\gamma$ are calculated from equations (1-3) and checked against the conditions of Tab. 1; if some type of error is likely to occur according to the process map, appropriate colors and symbols are displayed on a wireframe visualization of the triangle mesh (Fig. 11). The comparison with the actual edges on the part (Fig. 12) shows a good edge quality where the process map does not identify critical issues (detail A) and defects with clearly distinct morphology where the edges are classified as subject to staircase (detail B), radius (detail C) and support (detail D) effects.

## 5 Conclusions

Edges in AM parts have received little attention compared to surface features as regards geometric errors. Focusing on the FDM process, the paper has shown that additional variables (the included angle and the incidence angle) may have an influence on the quality of an edge compared to the well-known influence factors on surface quality (inclination angle and layer thickness). Accordingly, the analysis has highlighted some causes of geometric errors that are usually not considered for surfaces. They include edge-specific issues such as the radius effect, but also issues that may be further investigated for possible influences on surface quality, such as the offset, slicing and swelling effects.

As demonstrated in the example, the proposed process map can be useful as a diagnostic tool in a process planning procedure that considers a broader range of criteria than the currently known guidelines. For example, if edge quality is assumed as a further objective function for the optimization of build orientation, unexpected defects can be avoided with benefits on part function and appearance. In a scenario where the FDM process is used for short production runs, the results of the work could give rise to additional criteria for part design.

The limitations of the above reported results are mainly two. First, the error causes that justify the effects of the three geometric variables have been discussed according to general process knowledge, but their actual occurrence conditions have been assumed without an experimental verification. Secondly, no criterion has yet been formulated in order to predict the values of the position and form errors for edges with given combinations of associated angles. An experimental investigation will be reported in Part II to validate and extend the work.

## References


Agrawal S. and Dhande S.G. (2007), "Analysis of mechanical error in a fused deposition process using a stochastic approach", *International Journal of Production Research*, Vol. 45 No. 17, pp. 3991-4012.

Ahn D.K., Kim H.C. and Lee S.H. (2005), "Determination of fabrication direction to minimize post-machining in FDM by prediction of non-linear roughness characteristics", *Journal of Mechanical Science and Technology*, Vol. 19 No. 1, pp. 144-155.

Ahn D., Kweon J.H., Kwon S., Song J. and Lee S. (2009), "Representation of surface roughness in fused deposition modeling", *Journal of Materials Processing Technology*, Vol. 209, pp. 5593-5600.

Anitha R., Arunachalam S. and Radhakrishnan P. (2001), "Critical parameters influencing the quality of prototypes in fused deposition modelling", *Journal of Materials Processing Technology*, Vol. 118, pp. 385-388.

Bakar N.S.A., Alkahari M.R. and Boejang H. (2010), "Analysis on fused deposition modelling performance", *Journal of Zheijang University Science A*, Vol. 11 No. 12, pp. 972-977.

Boschetto A., Giordano V. and Veniali F. (2012), "Modelling micro geometrical profiles in fused deposition process", *International Journal of Advanced Manufacturing Technology*, Vol. 61, pp. 945-956.

Boschetto A., Giordano V. and Veniali F. (2013), "3D roughness profile model in fused deposition modelling", *Rapid Prototyping Journal*, Vol. 19 No. 4, pp. 240-252.

Boschetto A. and Bottini L. (2014), "Accuracy prediction in fused deposition modeling", *International Journal of Advanced Manufacturing Technology*, Vol. 73, pp. 913-928.

Boschetto A. and Bottini L. (2015), "Surface improvement of fused deposition modeling parts by barrel finishing", *Rapid Prototyping Journal*, Vol. 21 No. 6, pp. 686-696.

Campbell R.I., Martorelli M., Lee H.S. (2002), "Surface roughness visualisation for rapid prototyping models", Computer-Aided Design, Vol. 34, pp. 717-725.

Chang D.Y. and Huang B.H. (2011), "Studies on profile error and extruding aperture for the RP parts using the fused deposition modeling process", *International Journal of Advanced Manufacturing Technology*, Vol. 53, pp. 1027-1037.

Chen J.S.S. and Feng H.Y. (2011), "Contour generation for layered manufacturing with reduced part distortion", *International Journal of Advanced Manufacturing Technology*, Vol. 53, pp. 1103-1113.

Choi S.H. and Samavedam S. (2002), "Modelling and optimisation of rapid prototyping", *Computers in Industry*, Vol. 47, pp. 39-53.

Galantucci L.M., Lavecchia F., Percoco G. (2009), "Experimental study aiming to enhance the surface finish of fused deposition modeled parts", *CIRP Annals Manufacturing Technology*, Vol. 58, pp. 189-192.

Garg A., Bhattacharya A., Batish A. (2016), "On surface finish and dimensional accuracy of FDM parts after cold vapor treatment", *Materials and Manufacturing Processes*, Vol. 31 No. 4, pp. 522-529.

Ghorpade A., Karunakaran K.P. and Tiwan M.K. (2007), "Selection of optimal part orientation in fused deposition modelling using swarm intelligence", *Proceedings IMechE Part B: Journal of Engineering Manufacture*, Vol. 221, pp. 1209-1220.

Ingole D.S., Deshmukh T.R., Kuthe A.M. and Ashtankar K.M. (2011), "Build orientation analysis for minimum cost determination in FDM", *Proceedings IMechE Part B: Journal of Engineering Manufacture*, Vol. 225, pp. 1925-1938.

ISO 13715 (2000), "Technical drawings: edges of undefined shape, vocabulary and indications", International Organization for Standardization, Geneva, Switzerland.

Johnson W.J., Rowell M., Deason B. and Eubanks M. (2014), "Comparative evaluation of an open-source FDM system", *Rapid Prototyping Journal*, Vol. 20 No. 3, pp. 205-214.

Kantaros A. and Karalekas D. (2013), "Fiber Bragg grating based investigation of residual strains in ABS parts fabricated by fused deposition modeling process", *Materials and Design*, Vol. 50, pp. 44-50.

Kattethota G., Henderson M. (1998), "A tool to improve layered manufacturing part quality", Proceedings Solid Freeform Fabrication Symposium, Austin TX.

Lim T.Y. and Ratnam M.M. (2012), "Edge detection and measurement of nose radii of cutting tool inserts from scanned 2-D images", *Optics and Lasers in Engineering*, Vol. 50, pp. 1628-1642.

Mahapatra S.S. and Sood A.K. (2012), "Bayesian regularization-based Levenberg-Marquardt neural model combined with BFOA for improving surface finish of FDM processed parts", *International Journal of Advanced Manufacturing Technology*, Vol. 60, pp. 1223-1235.

Marsot J., Claudon L. and Jacqmin M. (2007), "Assessment of knife sharpness by means of a cutting force measuring system", *Applied Ergonomics*, Vol. 38, pp. 83-89.

Masood S.H., Rattanawong W. and Iovenitti P. (2000), "Part build orientations based on volumetric error in fused deposition modelling", *International Journal of Advanced Manufacturing Technology*, Vol. 16, pp. 162-168.

McCarthy C.T., Annaidh A.N. and Gilchrist M.D. (2010), "On the sharpness of straight edge blades in cutting soft solids: Part II – Analysis of blade geometry", *Engineering Fracture Mechanics*, Vol. 77 , pp. 437-451

Nancharaiah T., Raju R. and Raju V.R. (2010), "An experimental investigation on surface quality and dimensional accuracy of FDM components", *International Journal of Emerging Technologies*, Vol. 1 No. 2, pp. 106-111.

Noriega A., Blanco D., Alvarez B.J. and Garcia A. (2013), "Dimensional accuracy improvement of FDM square cross-section parts using artificial neural networks and an optimization algorithm", *International Journal of Advanced Manufacturing Technology*, Vol. 69, pp. 2301-2313.

Osawa S., Ito S., Shimizu Y., Jang S.H., Gao W., Fukuda T., Kato A. and Kubota K. (2012), "Cutting edge height measurement of a rotary cutting tool by a laser displacement sensor", *Journal of Advanced Mechanical Design, Systems and Manufacturing*, Vol. 6, pp. 815-828.

Pandey P.M., Venkata Reddy N., Dhande S.G. (2003), "Improvement of surface finish by staircase machining in fused deposition modeling", *Journal of Materials Processing Technology*, Vol. 132, pp. 323-331.

Peng A., Xiao X. and Yue R. (2014), "Process parameter optimization for fused deposition modeling using response surface methodology combined with fuzzy inference system", *International Journal of Advanced Manufacturing Technology*, Vol. 73, pp. 87-100.

Pérez C.J.L. (2002), "Analysis of the surface roughness and dimensional accuracy capability of fused deposition modelling processes", *International Journal of Production Research*, Vol. 40 No. 12, pp. 2865-2881.

Rattanawong W., Masood S.H. and Iovenitti P. (2001), "A volumetric approach to part-build orientations in rapid prototyping", *Journal of Materials Processing Technology*, Vol. 119, pp. 348-353.

Reilly G.A., McCormack B.A.O. and Taylor D. (2004), "Cutting sharpness measurement: a critical review", *Journal of Materials Processing Technology*, Vol. 153-154, pp. 261-267.

Singh R. (2014), "Process capability analysis of fused deposition modelling for plastic components", *Rapid Prototyping Journal*, Vol. 20 No. 1, pp. 69-76.

Sood A.K., Ohdar R.K. and Mahapatra S.S. (2009), "Parametric appraisal of fused deposition modelling process using the grey Taguchi method", *Proceedings IMechE Part B: Journal of Engineering Manufacture*, Vol. 224, pp. 135-145.

Tang W. (1993), "Cutting edge sharpness measurement using angle limited total integrated scattering", *Proceedings Industrial Electronics, Control and Instrumentation Conference*, Maui HI, pp. 1626-1628.

Taufik M., Jain P.K. (2016), "A study of build edge profile for prediction of surface roughness in fused deposition modeling", *ASME Journal of Manufacturing Science and Engineering*, Vol. 138, 061002.

Thrimurthulu K., Pandey P.M. and Reddy N.V. (2004), "Optimum part deposition orientation in fused deposition modeling", *International Journal of Machine Tools and Manufacture*, Vol. 44, pp. 585-594.

Tong K., Joshi S. and Lehtihet E.A. (2008), "Error compensation for fused deposition modeling (FDM) machine by correcting slice files", *Rapid Prototyping Journal*, Vol. 14 No. 1, pp. 4-14.

Turner B.N. and Gold S.A. (2015), "A review of melt extrusion additive manufacturing processes: II. Materials, dimensional accuracy and surface roughness", *Rapid Prototyping Journal*, Vol. 21 No. 3, pp. 250-261.

Volpato N., Foggiatto J.A. and Schwarz D.C. (2014), "The influence of support base on FDM accuracy in Z", *Rapid Prototyping Journal*, Vol. 20 No. 3, pp. 182-191.

Wang C.C., Lin T.W. and Hu S.S. (2007), "Optimizing the rapid prototyping process by integrating the Taguchi method with the Gray relational analysis", *Rapid Prototyping Journal*, Vol. 13 No. 5, pp. 304-315.

Wang T.M., Xi J.T. and Jin Y. (2007), "A model research for prototype warp deformation in the FDM process", *International Journal of Advanced Manufacturing Technology*, Vol. 33, pp. 1087-1096.

Xinhua L., Shengpeng L., Zhou L., Xianhua Z., Xiaohu C. and Zhongbin W. (2015), "An investigation on distortion of PLA thin-plate part in the FDM process", *International Journal of Advanced Manufacturing Technology*, Vol. 79 No. 5, pp. 1117-1126.

Zhang Y. and Chou K. (2008), "A parametric study of part distortions in fused deposition modelling using three-dimensional finite element analysis", *Proceedings IMechE Part B: Journal of Engineering Manufacture*, Vol. 222, pp. 959-967.

Ziemian C.W. and Crawn P.M. III (2001), "Computer aided decision support for fused deposition modeling", *Rapid Prototyping Journal*, Vol. 7 No. 3, pp. 138-147.

**List of figures**



**List of tables**

Part I – Tab. 1

| *Type of error* | *Effect* | *Condition* |
|---|---|---|
| Form | Staircase | $0° < \alpha < \theta_1$ |
| | Support | $90° - \gamma - \beta / 2 > \theta_2$ |
| Position | Radius | $\beta < \theta_3$ |
| | Offset | $\alpha > \theta_4$ |
| | Slicing, swelling | $\alpha = 0°$ |

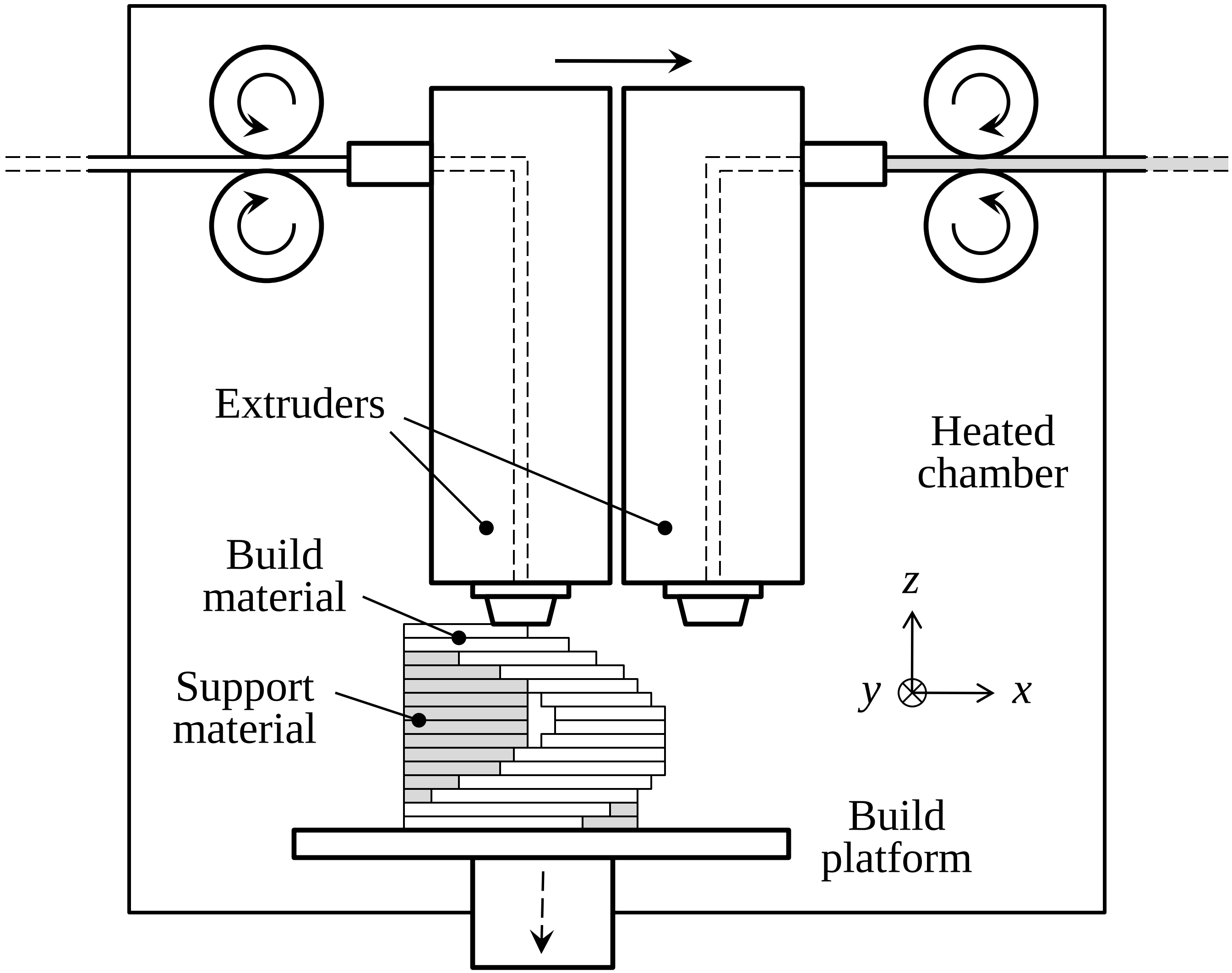
Extruders
Heated chamber
Build material
Support material
z
y
x
Build platform

Part I – Fig. 1

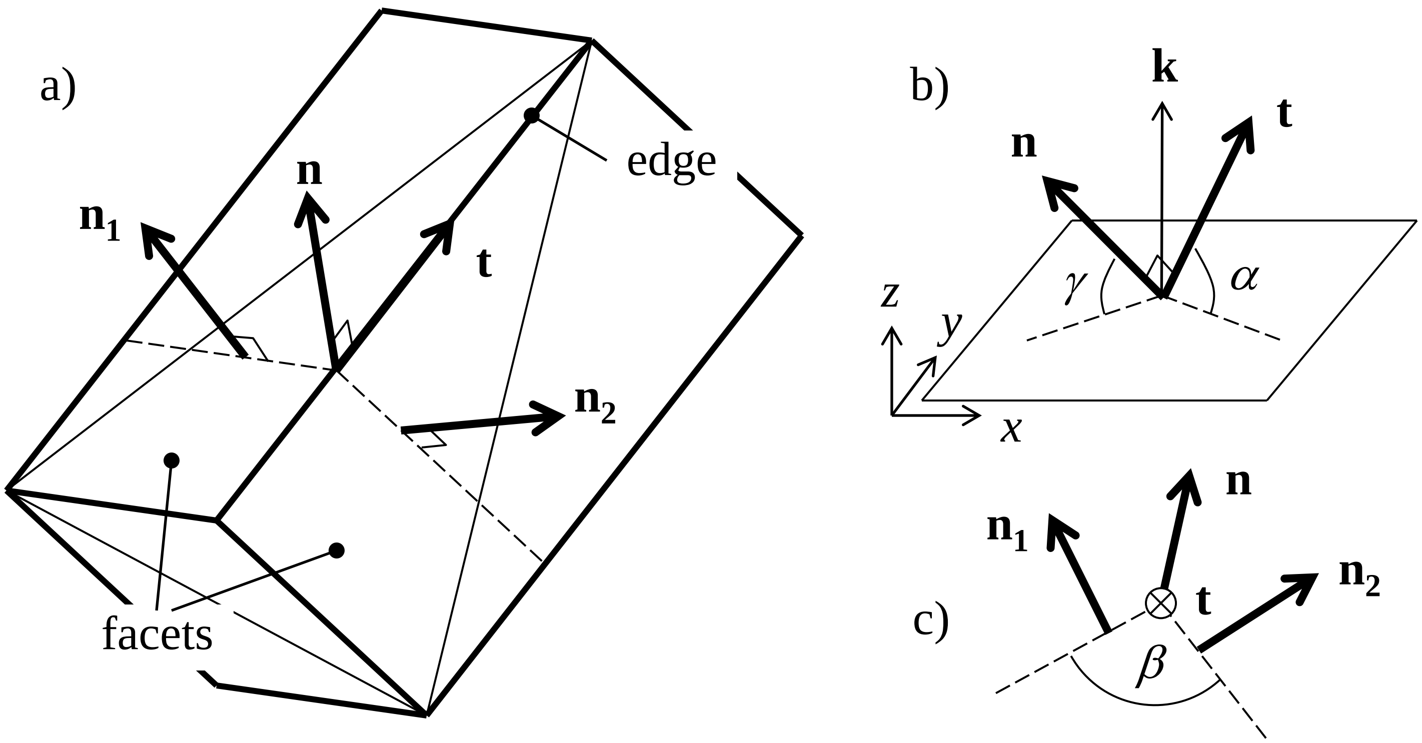


Part I – Fig. 2

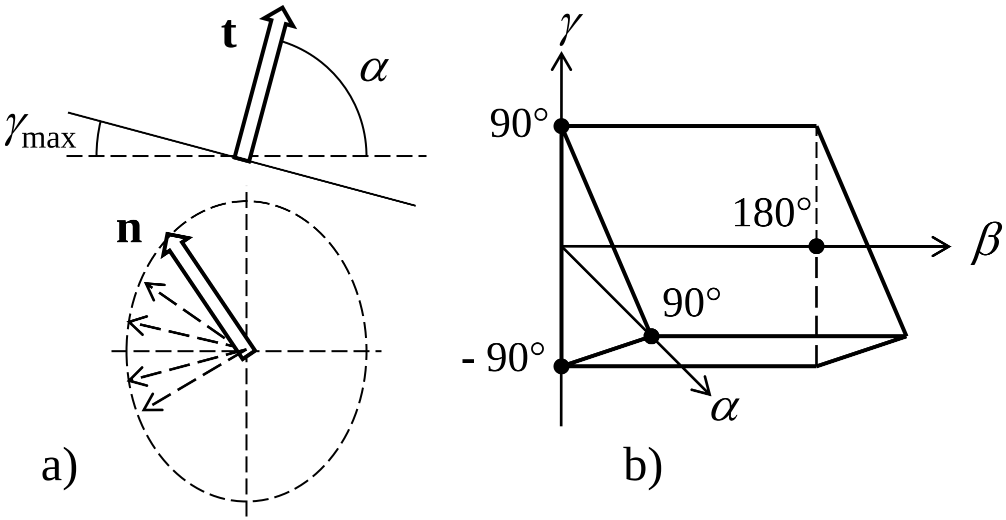


Part I – Fig. 3

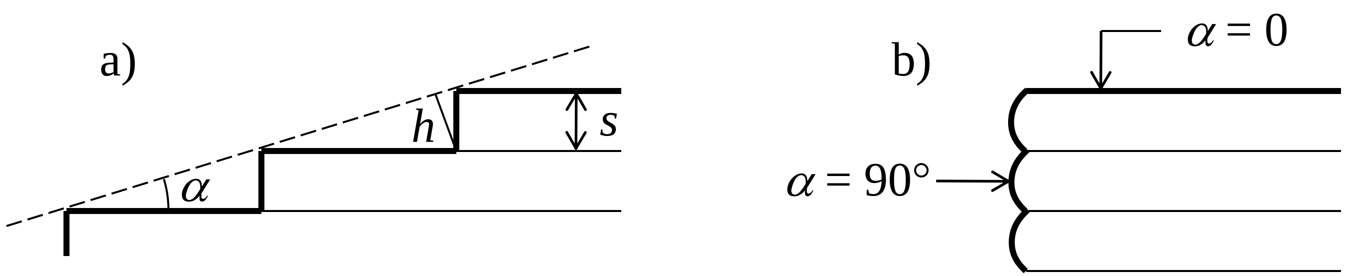


Part I – Fig. 4

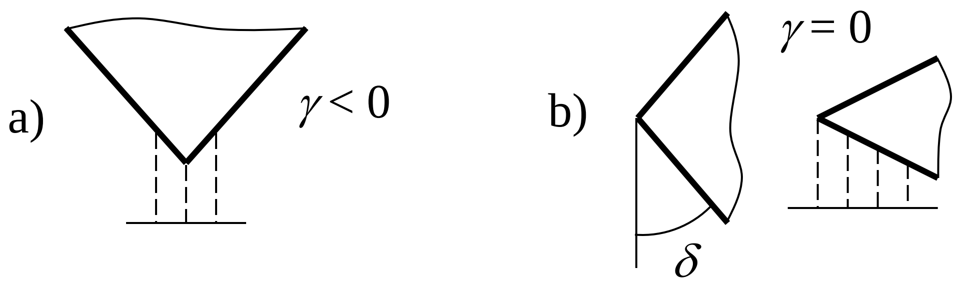


Part I – Fig. 5

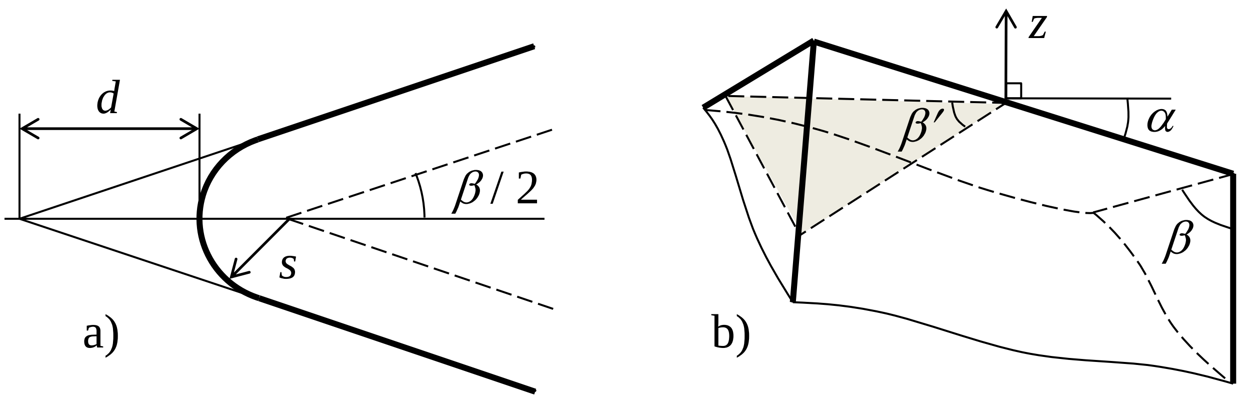


Part I – Fig. 6

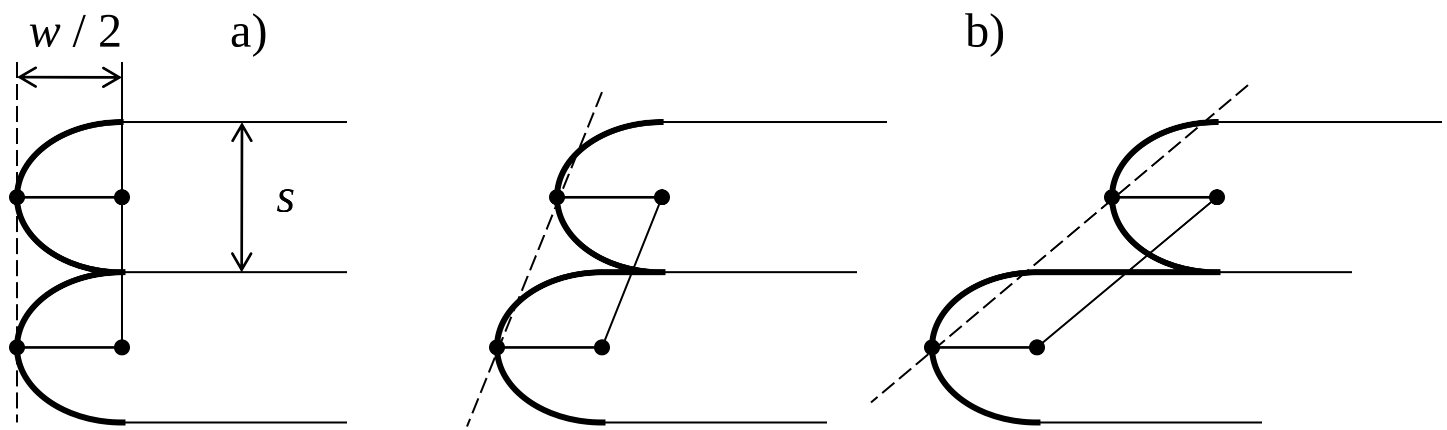


Part I – Fig. 7

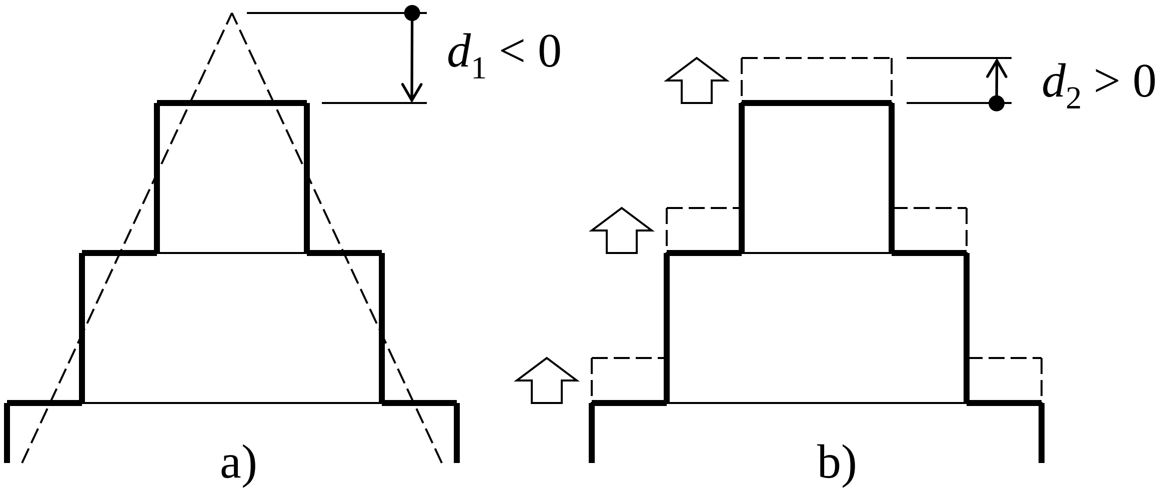


Part I – Fig. 8

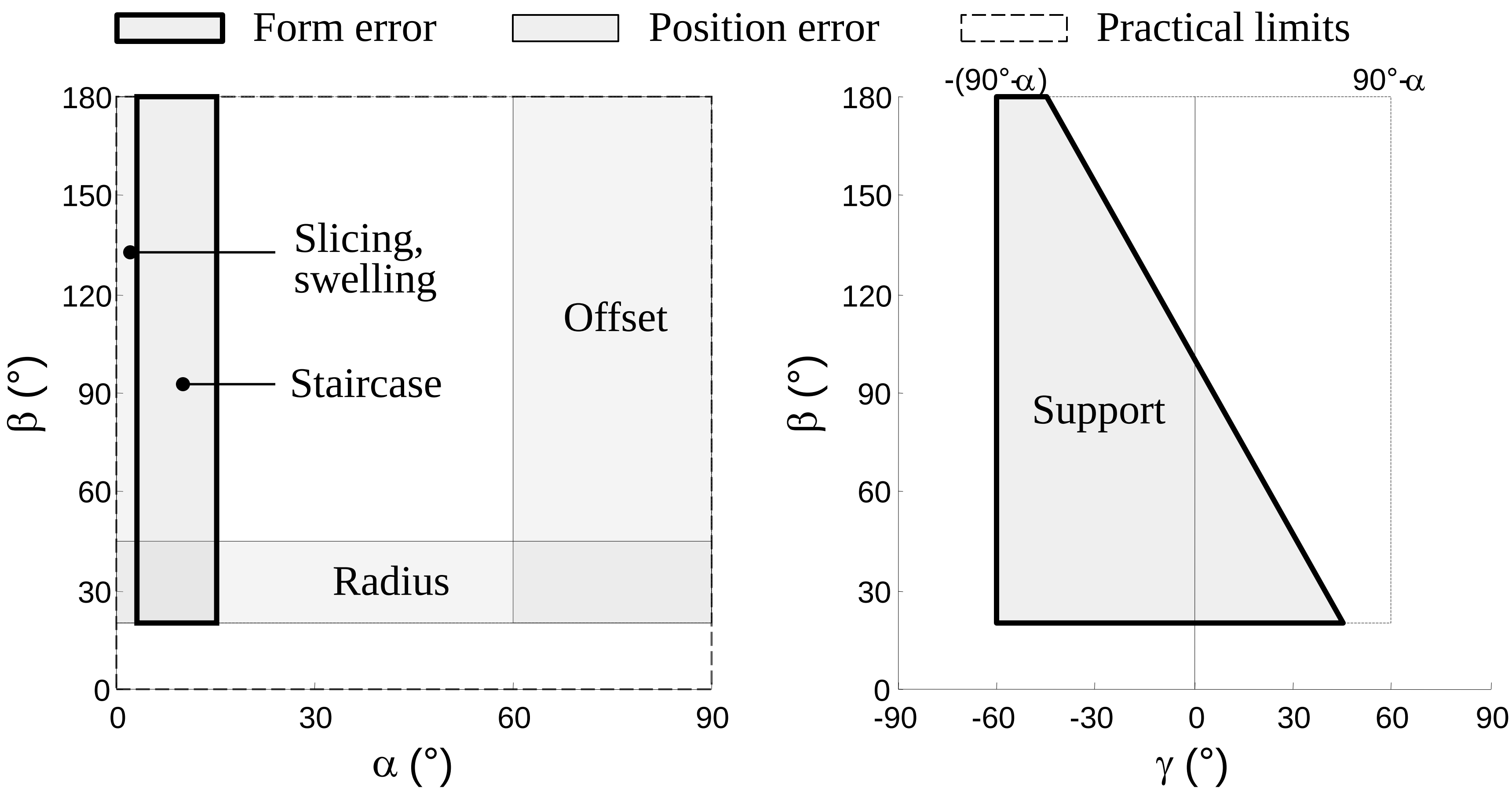
Form error
Position error
Practical limits
Slicing,
swelling
Staircase
Offset
Radius
β (°)
α (°)
-(90°-α)
90°-α
Support
β (°)
γ (°)

Part I – Fig. 9

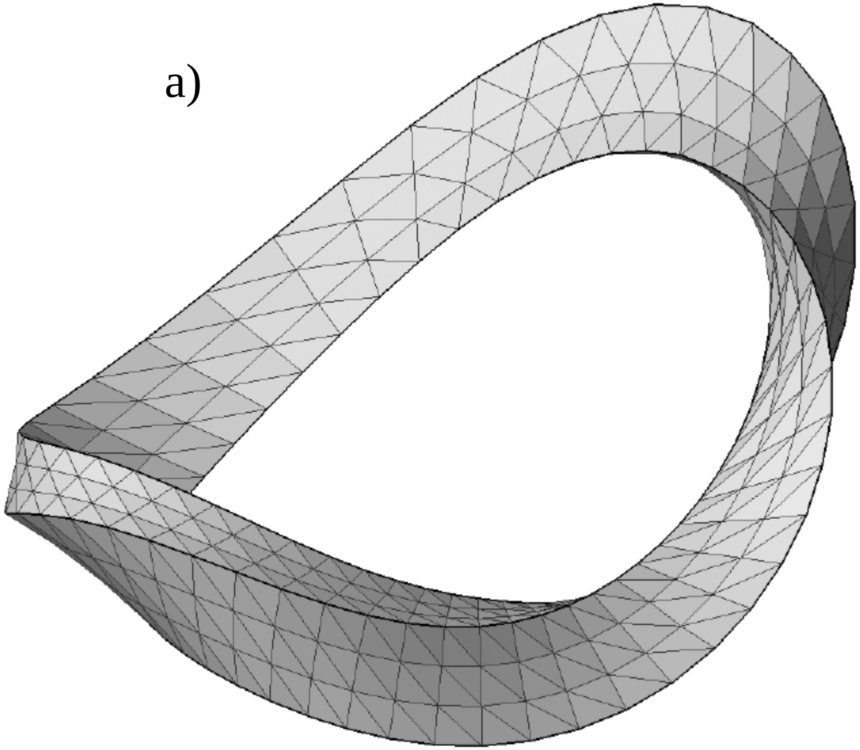


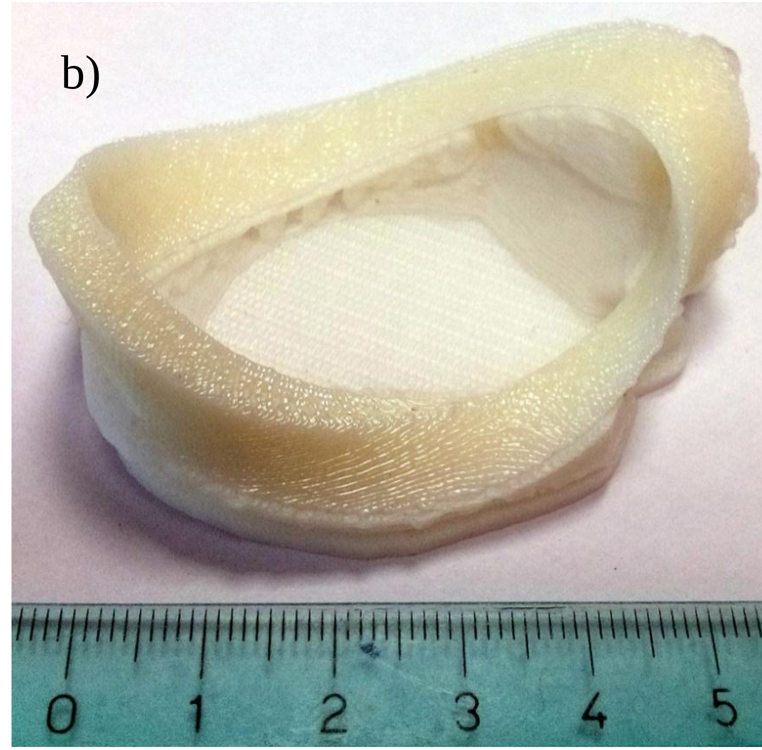


Part I – Fig. 10

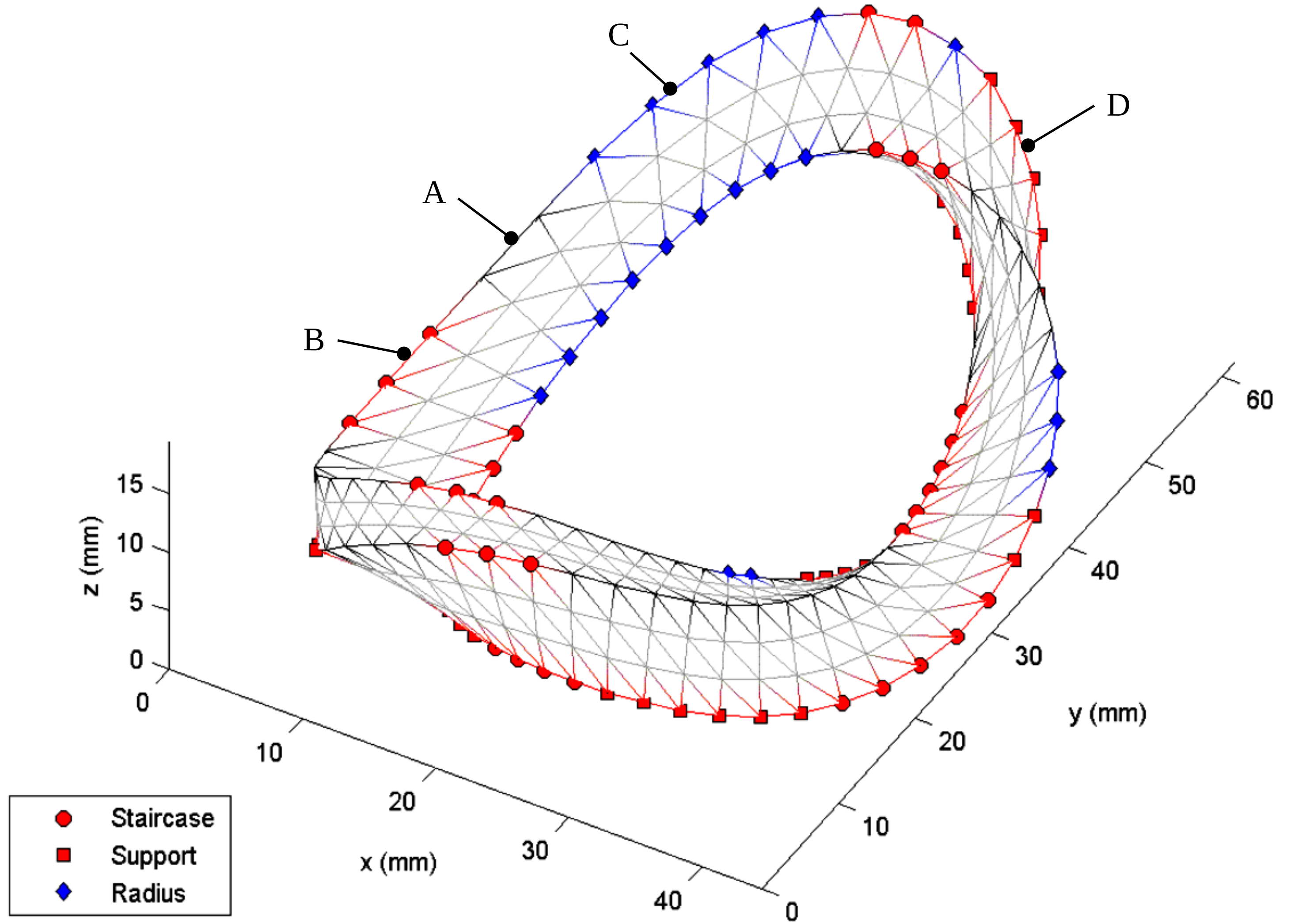
C
D
A
B
15
10
5
0
z (mm)
0
10
20
30
40
x (mm)
0
10
20
30
40
50
60
y (mm)
Staircase
Support
Radius

Part I – Fig. 11

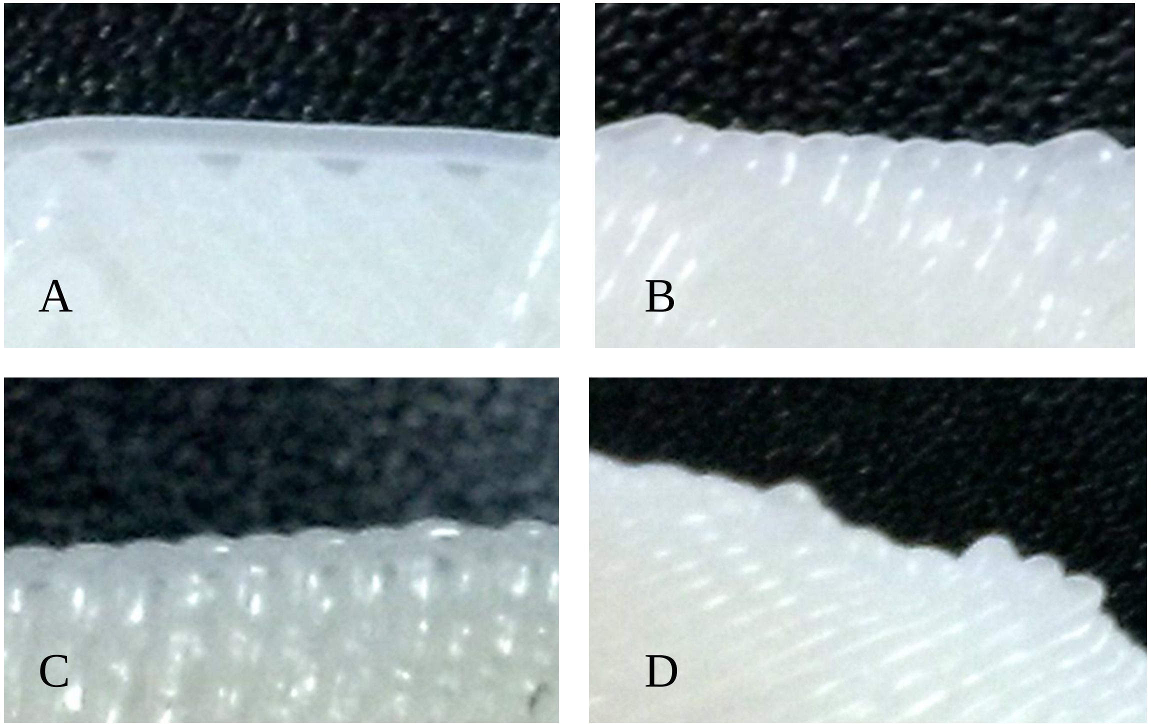


Part I – Fig. 12